Journal of Plant Growth Regulation (2023) 42:5842–5854
https://doi.org/10.1007/s00344-023-10969-2

Aminolevulinic Acid Coated—Silver, Copper, and Silver–Copper Nanoparticles: Synthesis, Characterization, and Application in Seed Nanopriming

Isabela S. Lopes[1] · **Flávia R. de O. Silva**[2] · **Lilia C. Courrol**[1,3]

Received: 9 September 2022 / Accepted: 24 February 2023 / Published online: 17 March 2023

Abstract

Seed priming is a potential tool for improving productivity under different environmental conditions. Aminolevulinic acid (ALA) priming can enhance plant tolerance to abiotic stresses, such as salinity, drought, and extreme temperatures. Nanopriming, priming with nanoparticles, can increase seed germination, growth, and plant development. The goal of this work was to compare the germination, growth, and development of sunflower seeds primed at 25 °C for 24 h with five treatments: water, ALA, silver, copper, and copper-silver nanoparticles (ALANPs) using a two-way analysis of variance. ALANPs were prepared by the photoreduction process (ALA as stabilizing/capping agent) and characterized by UV–Vis, transmission electron microscopy, FTIR, and Zeta potential. The germination percentage, shoot length, root length, seedling vigor index (Vi), and allometric coefficient were obtained on the 3rd, 6th, and 10th days after the priming process. The fluorescence spectra of chlorophyll extract of the whole seedling or directly in the cotyledons were measured. According to the results, seed priming with ALANPs enhanced sunflower seed germination capacity, seed growth, and increased chlorophyll production compared to water and ALA-primed seeds.

Keywords Metal nanoparticles · Aminolevulinic acid · Nanopriming, seed germination · Seed growth · Chlorophyll

Abbreviations

ALA	Aminolevulinic acid
ALANPs	Aminolevulinic acid-based nanoparticles
FTIR	Fourier-transform infrared
GP	Germination percentage
RL	Root length
SL	Shoot length
Vi	Vigor Index
AC	Allometric coefficient
PpIX	Protoporphyrin IX
ROS	Reactive oxygen species
PEG	Polyethylene glycol
ALAAgNPs	ALA:silver nanoparticles
ALACuNPs	ALA:copper nanoparticles
ALAAgCuNPs	Bimetallic ALA:silver-copper nanoparticles
PDI	Polydispersity index
TEM	Transmission electron microscopy
SPR	Surface plasmon resonance

Handling Editor: Jose M. Miguel.

✉ Lilia C. Courrol
lcourrol@unifesp.br

1 Programa de Pós-Graduação em Ciências e Tecnologia da Sustentabilidade, Universidade Federal de São Paulo, Diadema, São Paulo, Brazil

2 Centro de Ciências e Tecnologia dos Materiais, Instituto de Pesquisas Energéticas e Nucleares, IPEN/CNEN-SP, São Paulo, SP, Brazil

3 Instituto de Ciências Ambientais, Químicas e Farmacêuticas, Departamento de Física, Universidade Federal de São Paulo, Diadema, São Paulo, Brazil

Introduction

Sunflower (*Helianthus annuus L.)* is the world's fourth largest oil-producing crop after soybeans, rapeseed, and safflower (Adeleke and Babalola 2020; Bonciu et al. 2020). Furthermore, it is used as a raw material for biodiesel production (Tutunea et al. 2018). Sunflower seeds are dormant and germinate poorly, particularly at relatively low temperatures or temperatures > 45 °C, and under salt stress (Gay et al. 1991). This problem has been reported by many studies and is a bottleneck for the productivity of sunflowers

(El-Nwehy et al. 2018; Melnyk et al. 2020; Zhuykov et al. 2020; Sadiq et al. 2021; Sher et al. 2021). Studies also showed that seed priming could lighten these adverse effects (Akram et al. 2011; Catiempo et al. 2021; Silva et al. 2022).

Seed priming is a pre-sowing treatment in which seeds are immersed in a specific solution for a determined period (Marthandan et al. 2020). This process can boost the performance of crops in fragile ecosystems (Paparella et al. 2015). Hydropriming, hormonal priming, osmopriming, and biopriming are some of the priming methods that are used in these ecosystems (Nile et al. 2022). An innovative seed-priming method uses nanoparticles (NPs) as a priming agent. This method is known as nanopriming (Khalaki et al. 2021). The use of seed nanopriming in agriculture improves the quality of seeds and increases resistance against abiotic (heat or cold, drought or flood, salinity) and biotic stresses (microorganisms, insects, or weeds) (Mahakham et al. 2017; Santo Pereira et al. 2021). Nanopriming induces the formation of nanopores in the seed coat, which increases water uptake and activates reactive oxygen species (ROS), essential to breaking seed dormancy and promoting germination (Rai-Kalal et al. 2021; Silva et al. 2022).

Tan et al. reported that aminolevulinic acid (ALA) priming can activate nitric oxide, hydrogen peroxide, antioxidant capacity, osmoregulation, and nitrogen assimilation (Tan et al. 2022). ALA, a non-protein endogenous amino acid, is the first compound in the protoporphyrin IX (PpIX) synthesis pathway, which leads to heme synthesis in mammals and chlorophyll in plants. ALA is a crucial growth regulator in higher plants, and it has been proven to be effective in improving photosynthesis and alleviating the adverse effects of various abiotic stresses in higher plants (Wu et al. 2019; El-Shora et al. 2021).

In 1984 Rebeiz et al. reported that ALA could be used as an herbicide and insecticide (Rebeiz et al. 1984). The exogenous application of ALA in yeasts, insects, and plants induces a high accumulation of PpIX. PpIX is a generator of reactive oxygen species (ROS) when excited by light, in an appropriate wavelength, and in the presence of oxygen. ROS promotes cellular toxicity effects through apoptosis, necrosis, and autophagy. Under the action of PDT (photodynamic therapy) with sunlight, it is possible to perform pest control (Amindari et al. 1995). Studies focusing on alternative microbial production of ALA from renewable and inexpensive sources to increase production are underway, which justifies ALA use in agriculture (Zhang et al. 2015; Cui et al. 2019).

Aminolevulinic acid has been used to synthesize metallic nanoparticles by the photoreduction process (ALANPs) (Goncalves et al. 2015, 2018). In this process, the light is the reducing agent, and ALA acts as stabilizing/capping molecule since ALA structure has both a carboxylic acid group and an amino group, which are anchoring groups and aid in increasing binding strength and hence colloidal particle stability (Heuer-Jungemann et al. 2019). ALANPs are stable and potentialize the photodynamic activity of ALA (Goncalves et al. 2018, 2020; da Silva et al. 2021).

Silver and copper are the most studied metals for nanoparticle synthesis. Silver nanoparticles (AgNPs) have unique properties that protect seeds from bacteria and fungi and are potentially valuable for agricultural activities (Mishra and Singh 2015; Sahayaraj et al. 2015). AgNPs can stimulate seed germination by developing nanopores on the seed coat, activating reactive oxygen species (ROS), and promoting oxidative stress that is favorable for germination (Ethiraj and Kang 2012) Nile et al. 2022). Copper (Cu) is essential for plant growth (Gomes et al. 2021; Farooq et al. 2022). Seed priming with CuNPs positively impacts the initial development of seedlings (Gomes et al. 2021; Sarkar et al. 2021).

Therefore, this study was initiated with the objectives to evaluate a combination of nanoparticle type, size, composition, concentration, and chlorophyll content variation on sunflower seed germination after treatment with ALA nanoparticles synthesized by photoreduction process.

Materials and Methods

Silver, Copper, and Silver-Copper nanoparticles with 5-ALA synthesis

This study was conducted in the Applied Optical Biomedical Laboratory of the Department of Physics in the Federal University of São Paulo.

Silver nitrate, 5-Aminolevulinic acid hydrochloride ~98% (A3785), and Polyethylene glycol 10,000 (PEG) were purchased from Sigma-Aldrich. Cupric chloride dihydrate (99%) was purchased from Êxodo Científica (Brazil).

For ALAAgNPs synthesis, 1 mM of $AgNO_3$ (Sigma) was mixed with 6 mM of ALA (5-Aminolevulinic acid hydrochloride from Sigma) and 1 mol of Polyethylene Glycol (PEG) in distilled water at 20 °C. Then mixed and stirred vigorously. The solution was exposed to a 300 Watt Cermax Xenon lamp for 1 min (3.6 W/cm^2). After exposing for the irradiation, the solution was adjusted to pH 7.0 to improve stability for the suspension.

For the preparation of ALACuNPs, 6 mM of 5-ALA, 1 mM of $CuCl_{2,}$ and 1 M of PEG were diluted in distilled water and mixed thoroughly. Then, the solution was illuminated for 8 min. After the irradiation, the solution was adjusted to pH 7.0.

ALAAgCuNPs were synthesized by mixing 6 mM of 5-ALA, 1 mM of $AgNO_3$, 1 mM of $CuCl_{2,}$ and 1 mol of PEG in distilled water. The solution was illuminated for 5 min. After the brief irradiation, the solution was adjusted to pH 7.0.

Nanoparticles Characterization

The ultraviolet–visible (UV–Vis) absorption spectra was measured by a Shimadzu spectrophotometer using 10 mm quartz cells. The shape and sizes of ALANPs were determined with a transmission electron microscope (TEM) Jeol (Zeiss, Germany). The effective surface charges on the ALANPs were measured using Zeta potential (Malvern Instruments Zetasizer, Worcestershire, UK).

The Fourier-transform infrared spectroscopy (FTIR) spectra were obtained with a Shimadzu Prestige-21 spectrometer (Shimadzu Corp., Kyoto, JP) with a 2 cm^{-1} resolution range of 4000 to 400 cm^{-1}. The nanoparticles were dropped onto glass slides and left in the desiccator for 24 h. The dried material was used to prepare a KBr pellet for analysis.

Preparation of Seeds

The striped sunflower seeds (*Helianthus annuus* L.) were purchased from Danreal Indústria e Comércio Ltda, at São Paulo, Brazil. A Randomly selected seeds (with pericarp) were primed for 24 h and temperature of 25 ± 4 °C in 10 mL of water and different dilutions of ALA and ALANPs, to compare the germination, growth and at the same time toxicity traces. Five groups were studied: (1) Control group (water), (2) Aminolevulinic acid (ALA) solution group (6 mM-100%, 3 mM-50%, 1.5 mM-25% and 0.75 mM-12.5%), (3) ALAAgNPs group, (4) ALACuNPs group, and (5) ALAAgCuNPs group. For ALANPs groups, suspensions were studied without dilution (100%), and with distilled water dilutions of 50%, 25%, and 12.5%.

In Vitro Germination of Seeds

Primed seeds were collected 24 h after sowing and transferred to transparent plastic cups (diameter 7 cm) with lids lined with bond paper. The seeds ($n = 102$) were incubated at room temperature for 10 days in day/night conditions at 25 ±4°C. 1 mL of distilled water was added to the seeds every three days until the end of the experiment.

Measurement of Physiological Indices

Germination percentages ($GP = Ni/N \times 100$, where N is the total number of seeds and Ni is the number of germinated seeds), shoot length (SL), root length (RL), vigor index [$Vi = (RL + SL) \times GP$], and allometric coefficient ($AC = SL/RL$) were calculated on the 3rd, 6th, and 10th days after germination of nanoprimed seeds. Means and standard deviations were obtained from measurements on three replicates for each treatment. Seeds were considered germinated after the emergence of radicles from the seed coat.

Chlorophyll Fluorescence

On the 10th day after nanopriming, the two most vigorous samples of the studied group (considering that the water group has only two germinated seeds) were added to a falcon tube containing 5 mL of acetone and centrifugated for 15 min at 4000 rpm. The supernatant was measured in the fluorimeter Horiba Jobin Yvon-Fluorolog 3 with excitation at 434 nm, and the emission spectra were obtained between 550 and 750 nm. The chlorophyll measured in the whole seedling includes chlorophyll content in cotyledons and hypocotyls.

Also, the chlorophyll fluorescence was measured directly over the cotyledons using a bifurcated fiber outsider fluorimeter under excitation at 430 nm.

Effect of Hydrogen Peroxide (H_2O_2) in Nanoparticles

For this study 100 µL of H_2O_2 solutions (1 mM, 0.54 mM, 0.25 mM, 0.13 mM, 0.06 mM and 0.03 mM) were added in 1 mL of ALAAg, ALACu and ALAAgCuNPs solutions and the absorption spectrum was measured in UV–Vis region.

Statistical Analysis

A two-way analysis of variance (TI 84 type graphing calculator) was used to perform statistical analysis (p value < 0.05 was considered significant). Means and standard deviations were obtained from measurements on three replicates for the control and each treatment.

Results

Nanoparticles Characterization

UV–Vis and Zeta potential

The UV–Vis spectra of the synthesized nanoparticles are shown in Fig. 1. The surface plasmon resonance (SPR) of ALAAgNPs showed a peak centered near 437 nm at UV–Vis spectra (Fig. 1a), confirming the reduction of silver ions to colloidal silver. In Fig. 1b, the characteristic SPR spectra with absorbance at 620–710 nm can be attributed to the formation of ALACuNPs. Figure 1c shows the combined SPR bands of ALAAgCuNPs.

Table 1 presents the Zeta potential and polydispersity index values obtained for ALANPs. All nanoparticles were

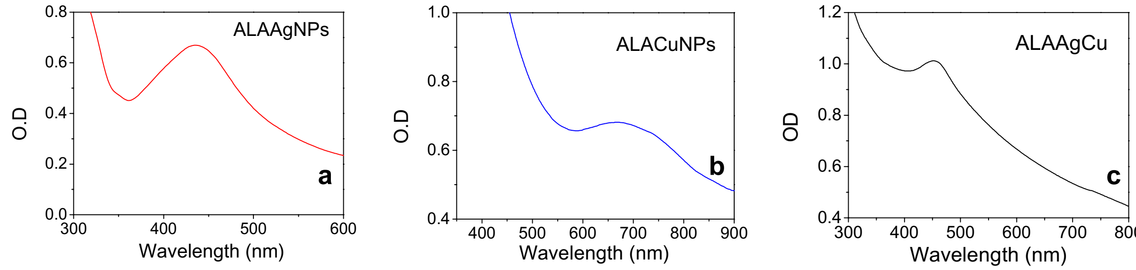

Fig. 1 UV–Vis spectra obtained for **a** ALAAgNPs, **b** ALACuNPs and **c** ALAAgCuNPs

Table 1 Zeta potential and polydispersity values obtained for ALAAg, ALACu, and ALAAgCuNPs

Sample	Zeta Potential (mV)	PDI
ALAAg	− 37.9	0.319
ALACu	− 24.4	0.361
ALAAgCu	− 16.3	0.505

negatively charged, and the ALAAg nanoparticles were presented the higher zeta potential value.

Fourier-Transform Infrared Spectroscopy (FTIR) Studies

The stability of colloidal suspension depends on the capping/ligand agents. ALA, in our case, serves as a capping agent. ALA presents amine (NH_2) and carboxyl (–COOH) functional groups. These two groups make bonds with metals through electrostatic interactions. ALA and ALANPs FTIR spectra are shown in Fig. 2.

FTIR spectrum of ALA presents bands in the region 4000–3000 cm^{-1} corresponding to the stretching vibrations of N–H and O–H. The band in the middle of the spectrum around 1720 cm^{-1} corresponds to the C=O stretch.

ALAAg exhibits peaks at 3436, 2882, 1727, 1342, 1278, 1239, 1120, 957, and 839 cm^{-1}. The band at 2882 cm^{-1} is related to the asymmetric stretching vibration of the C-H bond, and the band at 1343 cm^{-1} to the –O–H bending of carboxylates. The reduction of the intensity of C=O band from the carboxyl group (~ 1720 cm^{-1}) suggests strong interaction of the nanoparticles with this functional group.

ALACu nanoparticles present distinct peaks at 1594 cm^{-1} and 587 cm^{-1}. The ALAAgCuNPs spectrum is very similar to the ALACuNPs spectrum. The peak at 587 cm^{-1} is related

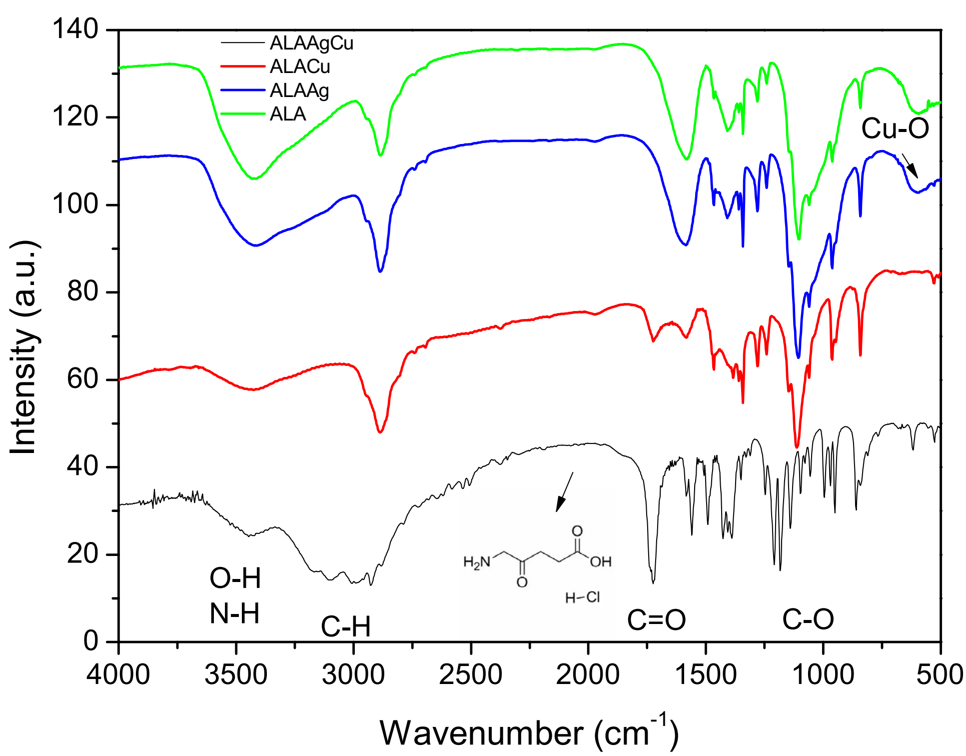

Fig. 2 FTIR spectra obtained for ALAAgNPs, ALACuNPs and ALAAgCuNPs

to the Cu–O bond, confirming the formation of CuNPs (Ethiraj and Kang 2012*)*. Carbonyl and hydroxyl groups are strongly attracted to copper oxide.

Transmission Electron Microscopy (TEM) Studies

The TEM images shown in Fig. 3 indicates that ALAAgNPs have sizes of around ~ 30 nm (Ag). ALACuNPs presented particles with sizes around 5 nm. ALAAgCuNPs consist of dispersed spherical nanoparticles with sizes of ~ 30 nm (Ag) and ~ 5 nm (Cu).

Seed Germination

Germination Rate, Root Length, Shoot Length, Vigor Index, and Allometric Coefficient

The seed germinates in three phases: Phase I Imbibition: seed hydration process; Phase II Activation: initiation of biochemical processes. Phase III Growth: initiation of growing processes. Primed seeds were removed from the priming solution in Phase II before the roots emerged.

Germination began during the second and third days after priming. Except for the hydropriming group, the remaining groups had recorded a germination percentage of 100%.

The images obtained on the 6th and 10th days are shown in Fig. 4. On the 6th day, enrolled hypocotyls were observed for ALA (12.5%) and ALANPs-primed seeds. One seed primed with ALA (100%) seeds had atrophied hypocotyls and another chlorotic coloring. On the 10th day, hypocotyls were disenrolled, and lateral roots and the green cotyledons were observed for ALANPs-treated seeds. Hydropriming seeds showed thin hypocotyl.

Nanopriming improved the speed of germination and vigor index, as observed in Fig. 5a and Table 1S. Vigor index showed progressive increase during the successive days. ALANPS significantly ($p < 0.05$) outperformed hydropriming treatment in vigor index after the 6th day. However, ALA (100%) showed lower vigor index compared to hydroprimed seedling treatment after the 6th day.

Figure 5b shows AC values in all groups in the 3rd, 6th, and 10th days after priming. There was no statistical difference between the groups, however, a reduction in AC values observed for ALANPs compared to the water group suggests that seed nanopriming positively impacts root growth as compared to shoot.

Chlorophyll Content

Figure 6a shows the excitation and emission spectra of chlorophyll (10th day) obtained directly from the cotyledons (excitation at 434 nm) or the whole seedling (excitation at 430 nm) primed with ALA. It is observed that the fluorescence in the cotyledons (684 nm) is red shifted compared to fluorescence obtained from chlorophyll extracted from the whole plant (669 nm). The excitation spectra obtained directly from cotyledons show the presence of bands Qx (one state of Q band) of chlorophyll *a* near 550 nm, and two overlapping Soret (B) bands are observed around 434 nm. The chlorophyll obtained from the whole plant is a composition between chlorophyll *a* and *b*.

Figure 6b compares the emission intensities of cotyledons chlorophyll of which group (water, ALA, ALAAg, ALACu, and ALAAgCu) indicating that intensity is higher for ALA primed seeds, but ALANPs present emission intensity higher than hydropriming seeds. A shift of chlorophyll maximum emission band from ~684 nm (ALA) to ~685 nm (ALACuNPs) was observed.

Figure 7 shows the fluorescence intensities of chlorophyll extract from the whole seedling in all the groups. The ALA and ALANPs primed seeds presented higher chlorophyll emission intensities than that obtained by water priming (green line) except for ALA (100%) and ALAAgCu (100%). A redshift in the maximum wavelength emission peak was observed in some spectra for ALAAg, ALACu, and ALAAgCu compared to the spectrum of water or ALA (Moreira et al. 2009).

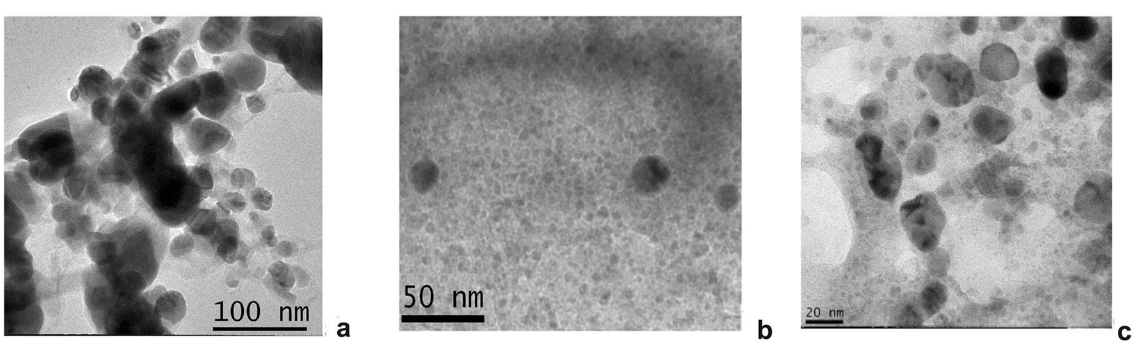

Fig. 3 TEM images of **a** ALAAgNPs, **b** ALACuNPs and **c** ALAAgCuNPs

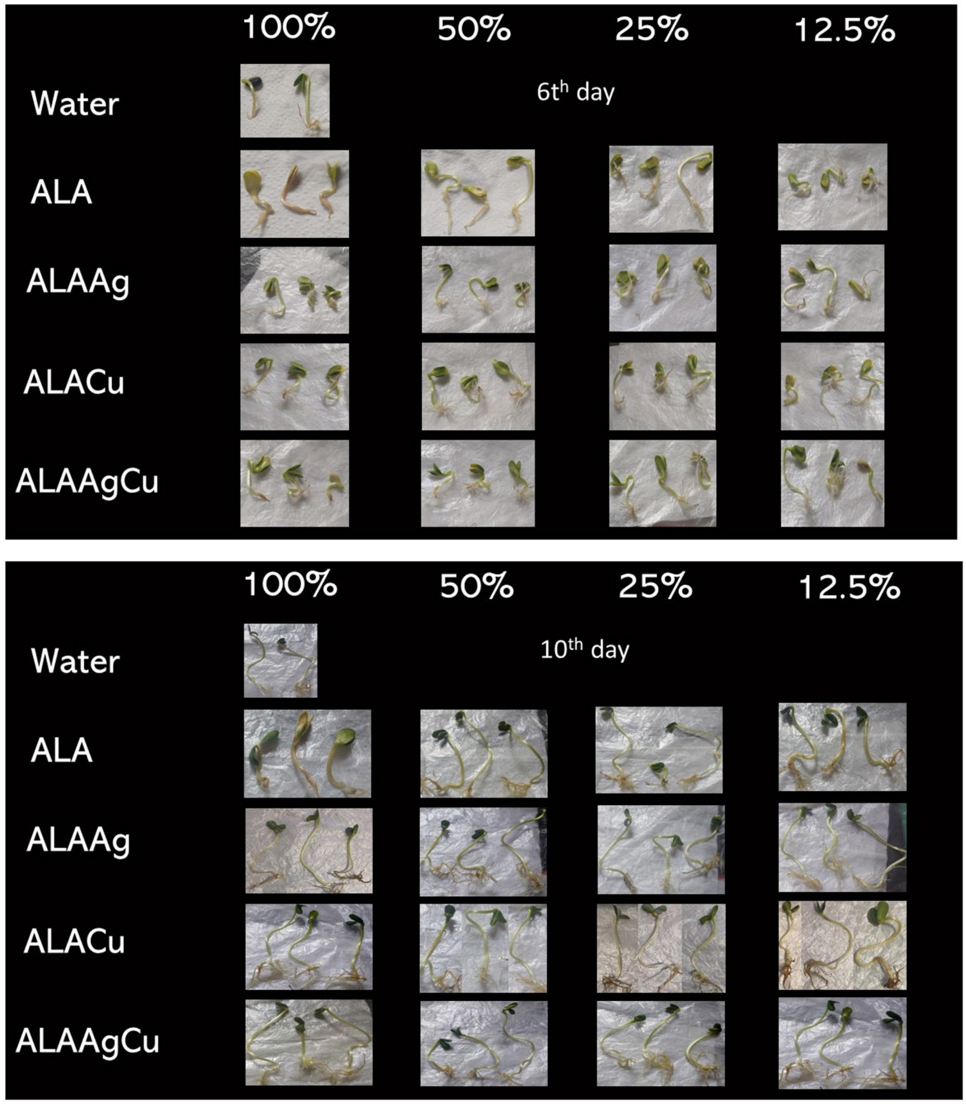

Fig. 4 The germination rate of sunflower seeds on the 6th and 10th days after priming with water, ALA, ALAAgNPs, ALA-CuNPs, and ALAAgCuNPs with 100, 50, 25, and 12.5% dilutions

Figure 8a compares the best values obtained for the vigor index (3rd, 6th, and 10th days). The results show that in all situations, ALA or ALANPs primed seeds presented better results than hydropriming seeds, and ALAAg and ALACu presented better results than ALA for vigor index. Vigor index on 3rd day for ALA and ALANPs group, compared with the water group, increased around 1.6 fold. On the 6th and 10th days, the ALA group increased by about 1.7-fold compared to the water group, while the increase was more than twofold for the ALAAgNPs group.

Figure 8b compares the best values obtained for the fluorescence intensity (669 nm) of chlorophyll extracted from samples (10th day) of controls and ALANPs groups. The fluorescence measurements indicated the best results for ALAAgCu primed seeds. ALA, ALAAg, ALACu, and ALAAgCu fluorescence intensities increased 1.4, 3.3, 3.2, and 4.2-folds, compared with the water group. So, the result indicated that ALANPs at least duplicated the seedling chlorophyll intensity compared to ALA.

Effect of ALANPs SPR Band in the Function of H_2O_2 Concentration

Figure 9a–c show UV–Vis spectra for (a) ALAAg, (b) ALACu, and (c) ALAAgCuNPs solutions measured after the priming process. Figure 9d, e, and f show the effect of increased H_2O_2 concentration over the ALAAg, ALACu, and ALAAgCu SPR bands. A decline in the SPR band was observed as H_2O_2 concentration increases. Similarly, NPs solution after 24 h priming, showed a similar decrease in SPR bands (Fig. 9a–c).

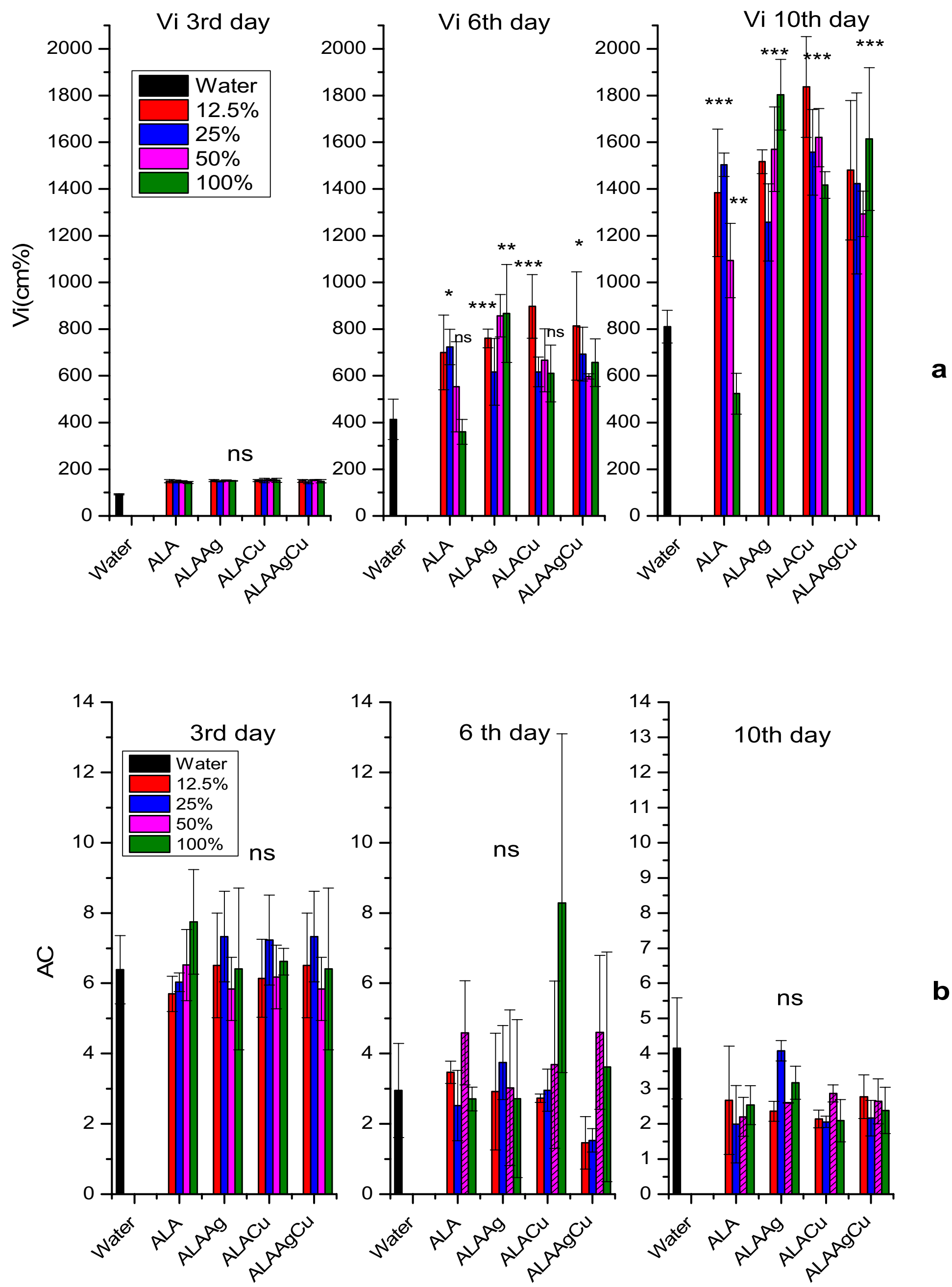

Fig. 5 **a** Vigor index (Vi) and **b** Allometric Coefficient (AC) obtained for water, ALA, ALAAg, ALACu, and ALAAgCu primed samples in 3rd, 6th and 10th days. *ns* non-significant; *significant at $p < 0.05$; **significant at $p < 0.01$; ***significant at $p < 0.001$

Discussion

In this work, sunflower seeds were subject to priming with water, ALA, and aminolevulinic acid nanoparticles. ALANPs synthesized by the photoreduction method presented good optical properties, stability, and sizes of around 5 nm (CuNPs) and 30 nm (AgNPs). Silver nanoparticles were more stable than copper or copper-silver nanoparticles. Indeed, copper has inherent instability under atmospheric conditions, which makes it prone to oxidation (Gawande et al. 2016).

Nanoparticles (NPs) interacted with the seed coat existing pores (1.6–4.6 nm), either enlarging those pores or forming new ones (Mishra and Singh 2015), which ultimately altered membrane fluidity. In the case of bimetallic ALAAgCuNPs we hypothesize that the smaller CuNPs interacted with the seed coat creating small dimples, that were enlarged by the AgNPs.

The stress imposed on the membrane by the presence of NPs probably induced the generation of hydrogen peroxide (H_2O_2) (Shin and Schachtman 2004). This process occurs once plasma membrane NADPH oxidase produces the superoxide anion ($O_2 - \bullet$) (Dynowski et al. 2008).

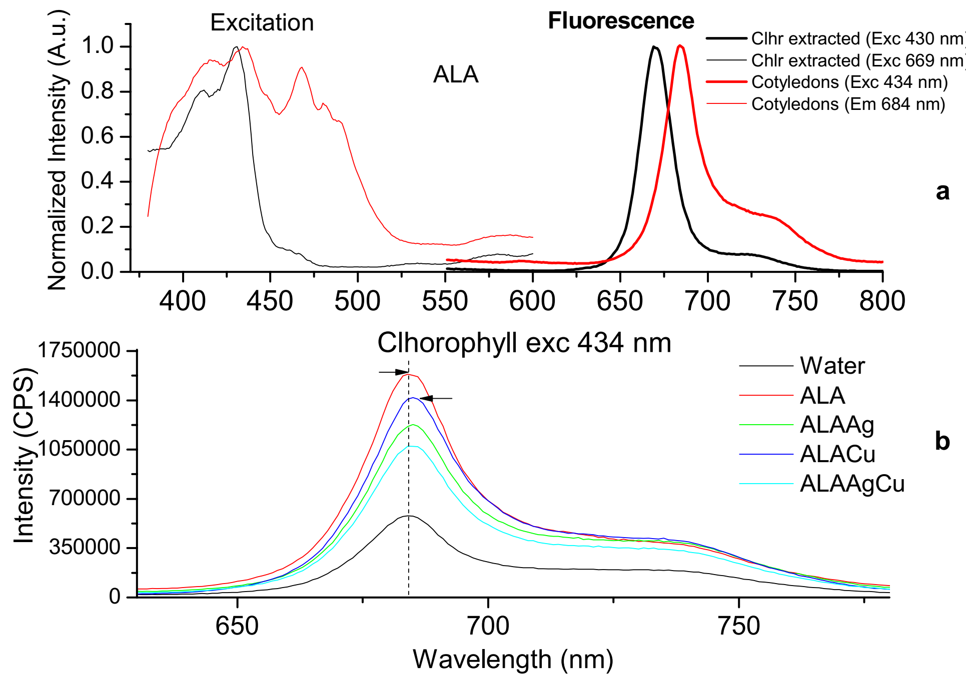

Fig. 6 **a** Excitation and fluorescence spectra obtained with excitation at 430 nm or 434 nm of chlorophyll extracted from seed primed with ALA compared with chlorophyll fluorescence obtained directly on the cotyledons, respectively. **b** Comparison between chlorophyll emission spectra in cotyledons of seeds primed with water, ALA, ALAAg, ALACu, and ALAAgCu

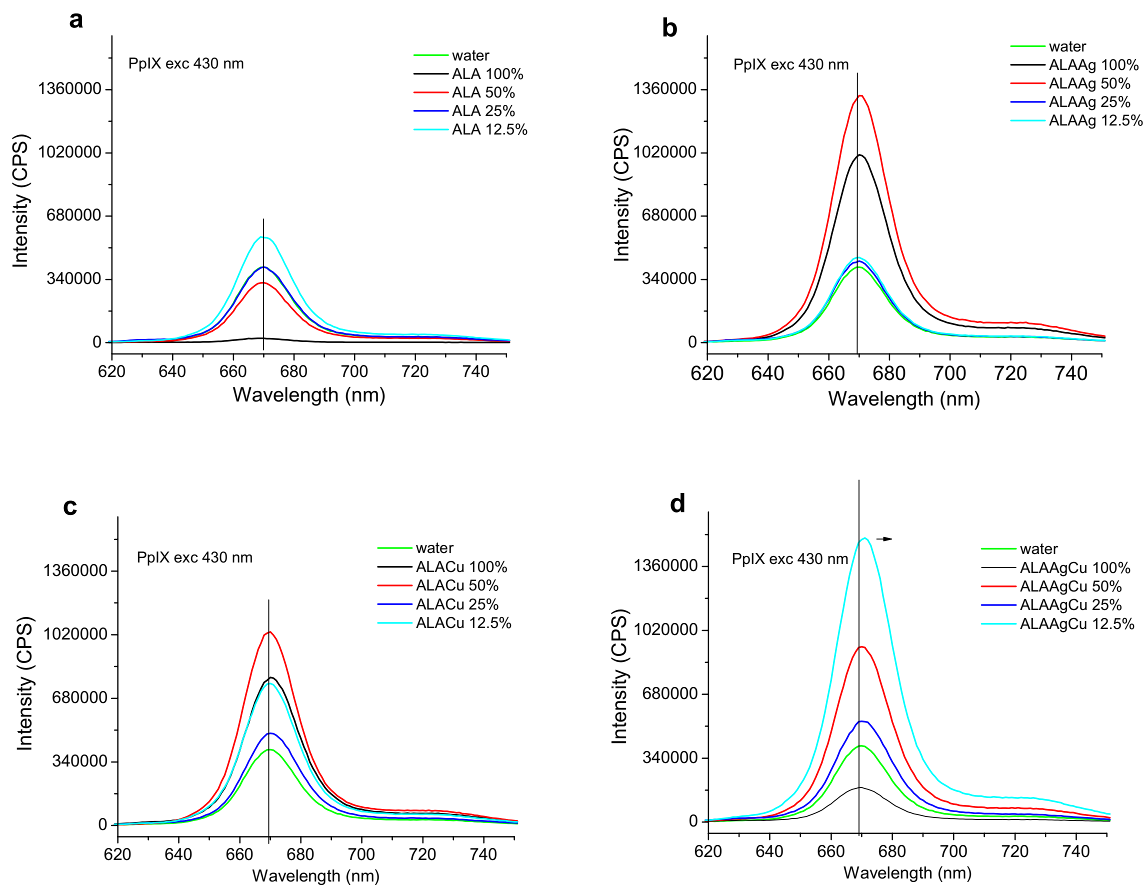

Fig. 7 Fluorescence spectra of chlorophyll extracted from two of the most vigorous seedlings obtained 10 days after priming from the studied groups: **a** ALA, **b** ALAAg, **c** ALACu, and **d** ALAAgCu

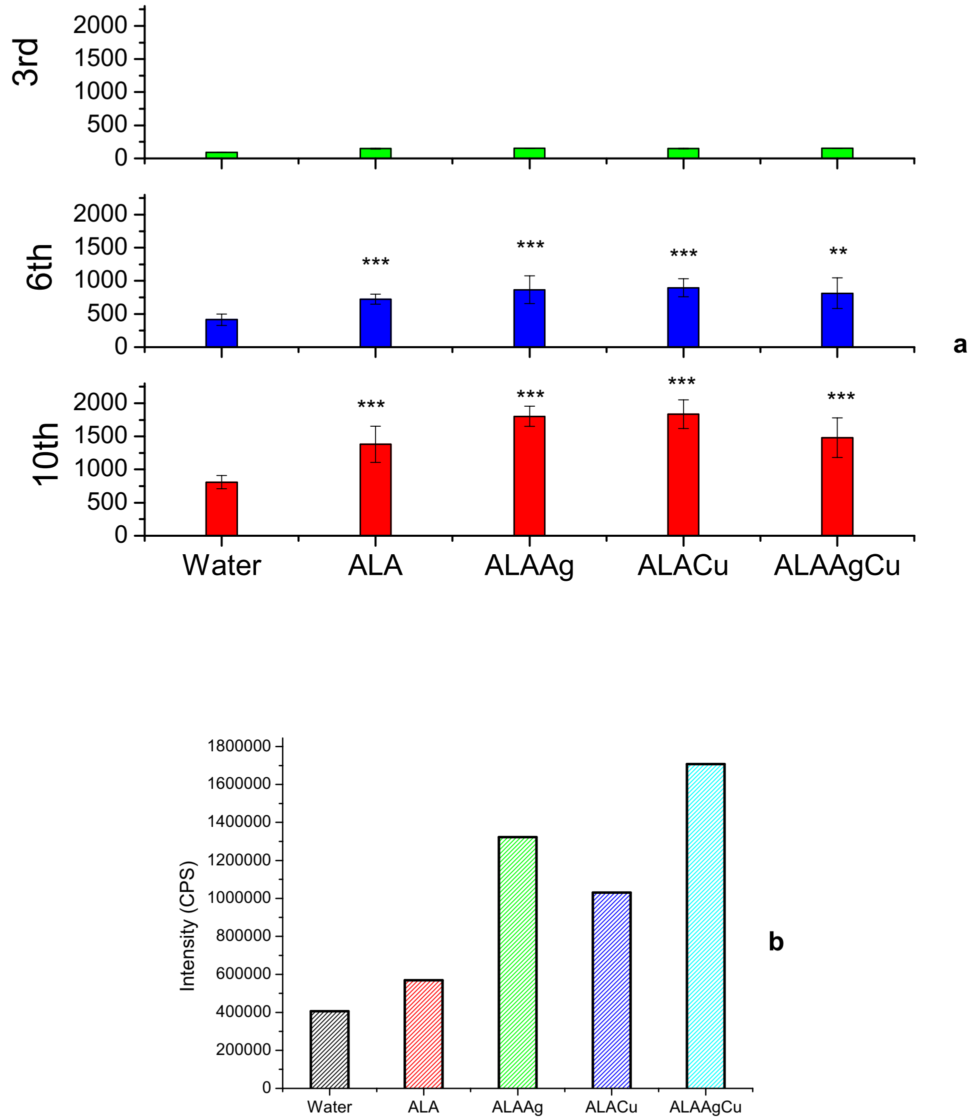

Fig. 8 Comparison between **a** Vi (3rd, 6th, and 10th days) and **b** fluorescence intensity (669 nm) of chlorophyll extracted from two samples (10th days) for water, ALA, ALAAg, ALACu, and ALAAgCu

Short-lived superoxide anions generate external H_2O_2. Plasma membrane aquaporins from plants facilitate the diffusion of H_2O_2 (Shin and Schachtman 2004).

The result showed in Fig. 9 indicated that after priming, nanoparticles were eliminated from the solutions. So, part of the NPs overcome the membrane, and part were dissociated in the primer solution. It is known that H_2O_2 is responsible for the dissolution of nanoparticles. We hypothesized that an increased concentration of H_2O_2 due to the induction of stress by NPs on the membrane led to the ALANPs dissociation forming metal ions and releasing ALA (Fig. 9d–f) (He et al. 2012; Mahakham et al. 2017; Zarif et al. 2020). ALA acted in chlorophyll metabolism while metal ions acted as essential micronutrients for normal plant metabolism (Sharma and Agrawal 2005; Krizkova et al. 2008).

Water uptake induced higher metabolic activity of seeds during the initial imbibition phase (Carpita et al. 1979) (Navarro et al. 2008). Mitochondria produces oxidative ATP by reducing molecular oxygen (O_2) to water in the electron transport chain. The superoxide radical produced in the mitochondria (Bailly et al. 2008) rapidly induces H_2O_2 which acted as a signaling molecule with phytohormones activating germination-related enzymes like α-amylase involved in the breaking of seed dormancy (Dayem et al. 2017; Rai-Kalal et al. 2021). The emergence of the radicle that occurred between two and three days after priming, except for the water group, was due to the formation of such enzymes.

Seeds primed with ALANPs lose their seed coat and pericarp more easily than ALA and water-primed seeds on the 6th day. As indicated in Fig. 4, on the sixth day, the hypocotyl emerged, and cotyledons became green. In the root part, secondary roots began, mainly in ALANPs primed seeds. On the 10th day, roots, hypocotyles, and green cotyledons undergone significant changes.

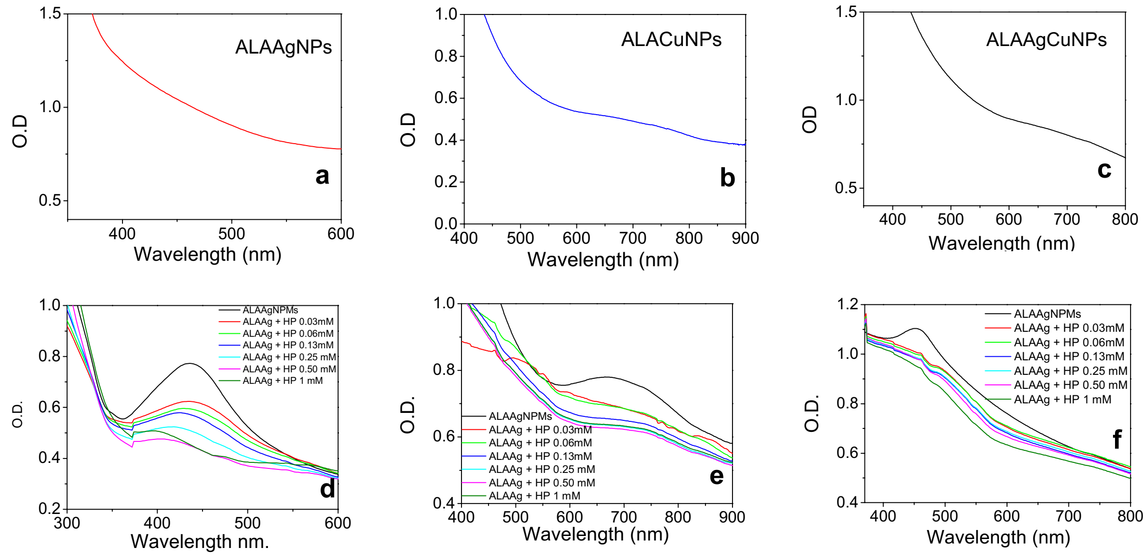

Fig. 9 UV–Vis spectra obtained for **a** ALAAgNPs, **b** ALACuNPs, and **c**)ALAAgCuNPs after removing seeds from solutions. Effect of increased concentration of H_2O_2 (1 Mm–0.03 mM) in **d** ALAAGNPs, **e** ALACuNPs and **f** ALAAgCuNPs

Seeds primed with ALANPs exhibited faster growth when compared to those hydroprimed treatments (Fig. 5), and this has been confirmed by similar studies (Younis et al. 2019; Thongmak et al. 2022). ALANPs increased seed germination and vigor index. The vigor index was improved after six days for ALACu (12.5%), ALAAg (100%), and ALAAgCu (12.5%). On the 10th day, the best results were obtained for ALAAg (100%) and ALACu (12.5%). Our study shows that NPs or silver ions released from the NPs did not result in toxicity to seedling and no oxidative damage to biological molecules was observed. However, copper ions in higher concentrations in ALACuNPs and ALAAgCuNPs resulted in lower values of vigor index.

ALA and ALANPs groups had reduced AC compared to the water group on the 10th day after priming (Fig. 5b). Seeds in these groups had longer roots and were visually more ramified.

ALA molecule on the surface of ALANPs was released inside the cell cytoplasm and metabolized to chlorophyll with insertion of magnesium ions (Mg^{2+}) in the PpIX structure(Reinbothe and Reinbothe 1996; Hotta et al. 1997; Akram and Ashraf 2011; Wu et al. 2019; Tan et al. 2022). The release of Ag^{2+} and Cu^{2+} ions with NPs dissolution, and same time an increased PpIX due to ALA, allowed beside chlorophyll also the chlorophyll-Ag^{2+} and chlorophyll-Cu^{2+} complexes production (Zengin and Kirbag 2007). In these cases, a shift in chlorophyll emission peak was observed (Fig. 5b), and the cotyledons presented a dark green color.

In cotyledons, only chlorophyll *a* was observed (Fig. 6). The chlorophyll emission spectra obtained from the whole seedling, cotyledons, and hypocotyles, (Fig. 7) indicated the presence of chlorophyll *a*, and *b*. Chlorophyll *a* is the principal pigment in photosynthesis, whereas chlorophyll *b* is the accessory pigment, collecting energy to pass into chlorophyll *a*. The redshift in the chlorophyll emission band in the ALAAg (50%) and ALAAgCu (25 and 12.5%), was probably due to magnesium replacement by silver or copper ions in the chlorophyll molecule.

The higher emission intensity of chlorophyll extracted from the seed was obtained from primed samples with ALAAg (50%) and ALAAgCu (12.5%), indicating that part of the chlorophyll was stored in hypocotyls to be used in stress conditions. Compared to the chlorophyll fluorescence intensity recorded directly from the cotyledons, ALA 100% was found to be lower than ALA 50%, 25%, and 12.5%. This result indicated that solutions containing high ALA concentration leaded to inhibition of chlorophyll probably due to the disequilibrium in ROS production (C. P. Zhang et al. 2013; Li et al. 2019). The low chlorophyll fluorescence intensity in the ALAAgCu (100%) could be due to the decrease in chlorophyll *a* and *b* and the increase in Ag or Cu contained chlorophyll molecules or toxicity caused by the presence of higher concentration of metal ions.

Figure 10 summarizes the priming process. Root development and enhancement in chlorophyll synthesis were improved by seed ALANPs priming. Besides, fast seed germination can enhance crop activity by stimulating the resistance of plants against abiotic and biotic stresses. This easy method has the potential to significantly improve the photosynthetic process of seedlings.

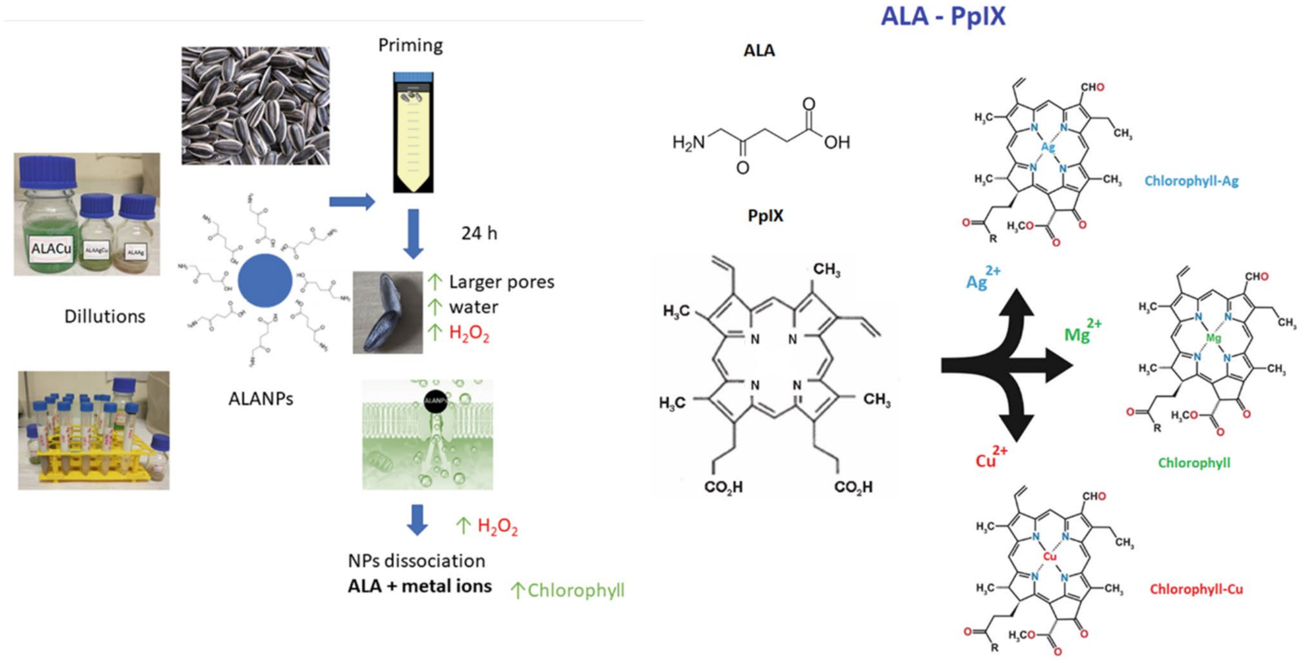

Fig. 10 ALANPs, dilutions, and steps of ALANPs priming: Nanoparticles enlarge the pores or form new pores on the seed coat and allow water uptake. ROS, mainly H_2O_2 outside and inside the cellular medium, dissociates ALANPs forming metal ions and releasing ALA. The chlorophyll content increase. Depending on NPs concentration, Mg^{2+} is substituted by Cu^{2+} or Ag^{2+} in the PpIX structure

Conclusions

Aminolevulinic acid nanoparticles (ALANPs) are easily synthesized using aminolevulinic acid and the photoreduction process by a clean and green method. ALANPs priming enhances the rate and percentage of seed germination, improves root growth, vigor, and increases chlorophyll content. ALANPs combine the effects of ALA and nanoparticles simultaneously. H_2O_2 generation in priming processes dissolves NPs releasing ALA and metal ions. Internalized NPs contribute to H_2O_2 generation, regulating seed dormancy and germination. The best results in terms of the vigor index compared with hydroprimed seeds were obtained with ALA (~1.7-fold), ALAAg (~2.2-fold), ALACu (~2.3-fold), and ALAAgCuNPs (~1.8-fold). Regarding chlorophyll content, ALA, ALAAg, ALACu, and ALAAgCu fluorescence intensities increased 1.4-fold, 3.3-fold, 3.2-fold, and 4.2-fold, respectively, compared with the water group. Silver and copper can replace the core magnesium ion in chlorophyll molecules, resulting in chlorophyll-metal complexes, and this was manifested by a shift in the chlorophyll emission band. Due to the characteristics of ALANPs, many other potential applications in agriculture are possible as fertilizers and pesticides, including the action of photodynamic activity. These systems can improve productivity and food quality, avoiding the drawbacks of conventional agriculture, and ensuring food security of farmers, consumers, and maintaining the sustainability of the environment.

Supplementary Information The online version contains supplementary material available at https://doi.org/10.1007/s00344-023-10969-2.

Acknowledgements From Brazil, the National Council for Scientific and Technological Development (CNPq – 465259/2014-6), the Coordination for the Improvement of Higher Education Personnel (CAPES), the National Institute of Science and Technology Complex Fluids (INCT-FCx), and the São Paulo Research Foundation (FAPESP – 2014/50983-3).

Author Contributions LCC designed the study and carried out the data analysis and interpretation of the results. ISL synthesized the ALANPS. FROS performed electronic microscopy analysis. All authors drafted the manuscript authors to read and approved the final manuscript.

Declarations

Conflict of interest The authors declare that there is no conflict of interest.

References

Adeleke BS, Babalola OO (2020) Oilseed crop sunflower (*Helianthus annuus*) as a source of food: nutritional and health benefits. Food Sci Nutr 8(9):4666–4684. https://doi.org/10.1002/fsn3.1783
Akram NA, Ashraf M (2011) Improvement in growth, chlorophyll pigments and photosynthetic performance in salt-stressed plants of

sunflower (*Helianthus annuus* L.) by foliar application of 5-aminolevulinic acid. Agrochimica 55(2):94–104
Akram NA, Ashraf M, Al-Qurainy F (2011) Aminolevulinic acid-induced changes in yield and seed-oil characteristics of sunflower (*Helianthus annuus* L.) plants under salt stress. Pak J Bot 43(6):2845–2852
Amindari S, Splittstoesser WE, Rebeiz CA (1995) Photodynamic effects of several metabolic tetrapyrroles on isolated chloroplasts. In: Heitz JR, Downum KR (eds) Light-activated pest control, vol 616. ACS publications, Washington D.C., pp 217–246
Bailly C, El-Maarouf-Bouteau H, Corbineau F (2008) From intracellular signaling networks to cell death: the dual role of reactive oxygen species in seed physiology. C R Biol 331(10):806–814. https://doi.org/10.1016/j.crvi.2008.07.022
Bonciu E, Pandia O, Olaru AL, Saracin I, Rosculete E (2020) Some aspects regarding the genetic and biotechnological progress of the *Helianthus annuus* L. Sci Papers-Series Manag Econ Eng Agric Rural Dev 20(1):105–110
Carpita N, Sabularse D, Montezinos D, Delmer DP (1979) Determination of the pore-size of cell-walls of living plant-cells. Science 205(4411):1144–1147. https://doi.org/10.1126/science.205.4411.1144
Catiempo RL, Photchanachai S, Bayogan ERV, Wongs-Aree C (2021) Impact of hydropriming on germination and seedling establishment of sunflower seeds at elevated temperature. Plant Soil Environ 67(9):491–498. https://doi.org/10.17221/163/2021-pse
Cui Z, Jiang Z, Zhang J, Zheng H, Jiang X, Gong K, Liang Q, Wang Q, Qi Q (2019) Stable and efficient biosynthesis of 5-aminolevulinic acid using plasmid-free *Escherichia coli*. J Agric Food Chem 67(5):1478–1483. https://doi.org/10.1021/acs.jafc.8b06496
da Silva R, Goncalves KD, Courrol LC, Caseli L (2021) Study of the interactions of gold nanoparticles functionalized with aminolevulinic acid in membrane models. Colloid Surfaces B-Biointerfaces. https://doi.org/10.1016/j.colsurfb.2021.111849
Dayem AA, Hossain MK, Lee SB, Kim K, Saha SK, Yang GM, Choi HY, Cho SG (2017) The role of reactive oxygen species (ROS) in the biological activities of metallic nanoparticles. Int J Mol Sci. https://doi.org/10.3390/ijms18010120
Dynowski M, Schaaf G, Loque D, Moran O, Ludewig U (2008) Plant plasma membrane water channels conduct the signalling molecule H_2O_2. Biochem J 414:53–61. https://doi.org/10.1042/bj20080287
El-Nwehy SS, El-Nasharty AB, Rezk AI (2018) Enhance sunflower productivity by foliar application of some plant growth bio-stimulants under salinity conditions. Biosci Res 15(3):1763–1768
El-Shora HM, Massoud GF, El-Sherbeny GA, Alrdahe SS, Darwish DB (2021) Alleviation of lead stress on sage plant by 5-Aminolevulinic Acid (ALA). Plants-Basel. https://doi.org/10.3390/plants10091969
Ethiraj AS, Kang DJ (2012) Synthesis and characterization of CuO nanowires by a simple wet chemical method. Nanoscale Res Lett. https://doi.org/10.1186/1556-276x-7-70
Farooq T, Nisa ZU, Hameed A, Ahmed T (2022) Priming with copper-chitosan nanoparticles elicit tolerance against PEG-induced hyperosmotic stress and salinity in wheat. BMC Chemistry. https://doi.org/10.1186/s13065-022-00813-1
Gawande MB, Goswami A, Felpin FX, Asefa T, Huang XX, Silva R, Zou XX, Zboril R, Varma RS (2016) Cu and Cu-based nanoparticles: synthesis and applications in review catalysis. Chem Rev 116(6):3722–3811. https://doi.org/10.1021/acs.chemrev.5b00482
Gay C, Corbineau F, Come D (1991) Effects Of temperature and oxygen on seed-germination and seedling growth in sunflower (*Helianthus annuus* L.). Environ Exp Bot 31(2):193–200. https://doi.org/10.1016/0098-8472(91)90070-5
Gomes DG, Pelegrino MT, Ferreira AS, Bazzo JHB, Zucareli C, Seabra AB, Oliveira HC (2021) Seed priming with copper-loaded chitosan nanoparticles promotes early growth and enzymatic antioxidant defense of maize (*Zea mays* L.) seedlings. J Chem Technol Biotechnol 96(8):2176–2184. https://doi.org/10.1002/jctb.6738
Goncalves KD, Cordeiro TD, Silva FRD, Samad RE, Vieira ND, Courrol LC (2015, May 23-25). Preparation and optimization of aminolevulinic acid with gold nanoparticles for photothermal and photodynamic therapies applications. Paper presented at the Joint Meeting of the 1st SPIE Conference on Biophotonics South America (BSA)/15th World Congress of the International-Photodynamic-Association (IPA), Rio de Janeiro, Brazil
Goncalves KD, Vieira DP, Courrol LC (2018) Synthesis and characterization of aminolevulinic acid gold nanoparticles: photo and sonosensitizer agent for atherosclerosis. J Lumin 197:317–323. https://doi.org/10.1016/j.jlumin.2018.01.057
Goncalves KD, Vieira DP, Levy D, Bydlowski SP, Courrol LC (2020) Uptake of silver, gold, and hybrids silver-iron, gold-iron and silver-gold aminolevulinic acid nanoparticles by MCF-7 breast cancer cells. Photodiagn Photodyn Ther. https://doi.org/10.1016/j.pdpdt.2020.102080
He D, Garg S, Waite TD (2012) H_2O_2-mediated oxidation of zero-valent silver and resultant interactions among silver nanoparticles, silver ions, and reactive oxygen species. Langmuir 28(27):10266–10275. https://doi.org/10.1021/la300929g
Heuer-Jungemann A, Feliu N, Bakaimi I, Hamaly M, Alkilany A, Chakraborty I, Masood A, Casula MF, Kostopoulou A, Oh E, Susumu K, Stewart MH, Medintz IL, Stratakis E, Parak WJ, Kanaras AG (2019) The role of ligands in the chemical synthesis and applications of inorganic nanoparticles. Chem Rev 119(8):4819–4880. https://doi.org/10.1021/acs.chemrev.8b00733
Hotta Y, Tanaka T, Takaoka H, Takeuchi Y, Konnai M (1997) New physiological effects of 5-aminolevulinic acid in plants: the increase of photosynthesis, chlorophyll content, and plant growth. Biosci Biotechnol Biochem 61(12):2025–2028. https://doi.org/10.1271/bbb.61.2025
Khalaki MA, Moameri M, Lajayer BA, Astatkie T (2021) Influence of nano-priming on seed germination and plant growth of forage and medicinal plants. Plant Growth Regul 93(1):13–28. https://doi.org/10.1007/s10725-020-00670-9
Krizkova S, Ryant P, Krystofova O, Adam V, Galiova M, Beklova M, Babula P, Kaiser J, Novotny K, Novotny J, Liska M, Malina R, Zehnalek J, Hubalek J, Havel L, Kizek R (2008) Multi-instrumental analysis of tissues of sunflower plants treated with silver(I) ions—Plants as bioindicators of environmental pollution. Sensors 8(1):445–463. https://doi.org/10.3390/s8010445
Li JJ, Yang C, Liu H, Cao MT, Yan GJ, Si P, Zhou WJ, Xu L (2019) 5-aminolevolinic acid enhances sunflower resistance to *Orobanche cumana* (Broomrape). Ind Crops Prod. https://doi.org/10.1016/j.indcrop.2019.111467
Mahakham W, Sarmah AK, Maensiri S, Theerakulpisut P (2017) Nanopriming technology for enhancing germination and starch metabolism of aged rice seeds using phytosynthesized silver nanoparticles. Sci Rep. https://doi.org/10.1038/s41598-017-08669-5
Marthandan V, Geetha R, Kumutha K, Renganathan VG, Karthikeyan A, Ramalingam J (2020) Seed priming: a feasible strategy to enhance drought tolerance in crop plants. Int J Mol Sci. https://doi.org/10.3390/ijms21218258
Melnyk A, Akuaku J, Melnyk T, Makarchuk A (2020) Influence of photosynthetic apparatus on the productivity of high-oleic sunflower depending on climatic conditions in the left-bank forest-steppe of Ukraine. Bulgarian J Agr Sci 26(4):800–808
Mishra S, Singh HB (2015) Biosynthesized silver nanoparticles as a nanoweapon against phytopathogens: exploring their scope and potential in agriculture. Appl Microbiol Biotechnol 99(3):1097–1107. https://doi.org/10.1007/s00253-014-6296-0
Moreira LM, Lima A, Soares RRS, Batistela VR, Gerola AP, Hioka N, Bonacin JA, Severino D, Baptista MS, Machado AED, Rodrigues

MR, Codognoto L, de Oliveira HPM (2009) Metallochlorophylls of magnesium, copper and zinc: evaluation of the influence of the first coordination sphere on their solvatochromism and aggregation properties. J Braz Chem Soc 20(9):1653–1658. https://doi.org/10.1590/s0103-50532009000900013
Navarro E, Baun A, Behra R, Hartmann NB, Filser J, Miao AJ, Quigg A, Santschi PH, Sigg L (2008) Environmental behavior and ecotoxicity of engineered nanoparticles to algae, plants, and fungi. Ecotoxicology 17(5):372–386. https://doi.org/10.1007/s10646-008-0214-0
Nile SH, Thiruvengadam M, Wang Y, Samynathan R, Shariati MA, Rebezov M, Nile A, Sun MH, Venkidasamy B, Xiao JB, Kai GY (2022) Nano-priming as emerging seed priming technology for sustainable agriculture-recent developments and future perspectives. J Nanobiotechnol. https://doi.org/10.1186/s12951-022-01423-8
Paparella S, Araujo SS, Rossi G, Wijayasinghe M, Carbonera D, Balestrazzi A (2015) Seed priming: state of the art and new perspectives. Plant Cell Rep 34(8):1281–1293. https://doi.org/10.1007/s00299-015-1784-y
Rai-Kalal P, Tomar RS, Jajoo A (2021) H_2O_2 signaling regulates seed germination in ZnO nanoprimed wheat (*Triticum aestivum* L.) seeds for improving plant performance under drought stress. Environ Exp Bot. https://doi.org/10.1016/j.envexpbot.2021.104561
Rebeiz CA, Montazerzouhoor A, Hopen HJ, Wu SM (1984) Photodynamic herbicides: 1 concept and phenomenology. Enzyme Microb Technol 6(9):390–401. https://doi.org/10.1016/0141-0229(84)90012-7
Reinbothe S, Reinbothe C (1996) The regulation of enzymes involved in chlorophyll biosynthesis. Eur J Biochem 237(2):323–343. https://doi.org/10.1111/j.1432-1033.1996.00323.x
Sadiq M, Mazhar U, Shah GA, Hassan Z, Iqbal Z, Mahmood I, Wattoo FM, Niazi MBK, Bran A, Arthur K, Ali N, Rashid MI (2021) Zinc plus biopolymer coating slows nitrogen release, decreases ammonia volatilization from urea and improves sunflower productivity. Polymers. https://doi.org/10.3390/polym13183170
Sahayaraj K, Roobadevi M, Rajesh S, Azizi S (2015) *Vernonia cinerea* (L.) Less. silver nanocomposite and its antibacterial activity against a cotton pathogen. Res Chem Intermed 41(8):5495–5507. https://doi.org/10.1007/s11164-014-1676-8
Sarkar N, Sharma RS, Kaushik M (2021) Innovative application of facile single pot green synthesized CuO and CuO@APTES nanoparticles in nanopriming of *Vigna radiata* seeds. Environ Sci Pollut Res 28(11):13221–13228. https://doi.org/10.1007/s11356-020-11493-6
Sharma RK, Agrawal M (2005) Biological effects of heavy metals: an overview. J Environ Biol 26(2):301–313
Sher A, Arfat MY, Ul-Allah S, Sattar A, Ijaz M, Manaf A, Qayyum A, Zuan ATK, Nasif O, Gasparovic K (2021) Conservation tillage improves productivity of sunflower (*Helianthus annuus* L.) under reduced irrigation on sandy loam soil. PLoS ONE. https://doi.org/10.1371/journal.pone.0260673
Shin R, Schachtman DP (2004) Hydrogen peroxide mediates plant root cell response to nutrient deprivation. Proc Natl Acad Sci USA 101(23):8827–8832. https://doi.org/10.1073/pnas.0401707101
Silva PCC, Neto ADA, Gheyi HR, Ribas RF, Silva CRR, Cova AMW (2022) Seed priming with H2O2 improves photosynthetic efficiency and biomass production in sunflower plants under salt stress. Arid Land Res Manag 36(3):283–297. https://doi.org/10.1080/15324982.2021.1994482
Tan SY, Cao J, Xia XL, Li ZH (2022) Advances in 5-aminolevulinic acid priming to enhance plant tolerance to abiotic stress. Int J Mol Sci. https://doi.org/10.3390/ijms23020702
Thongmak W, Ruangwong K, Wongkaew A, Srisonphan S, Onwimol D (2022) Responses of seed vigour and germination of maize to plasma-activated water priming, silver-nanopriming and green silver-nanopriming. Seed Sci Technol 50(1–3):117–131. https://doi.org/10.15258/sst.2022.50.1.10
Tutunea D, Dumitru I, Racila L, Otat O, Matei L, Geonea I (2018) Characterization of Sunflower Oil Biodiesel as Alternative for Diesel Fuel. Paper presented at the 4th International Congress of Automotive and Transport Engineering (AMMA), Cluj-Napoca, Romania
Wu Y, Liao WB, Dawuda MM, Hu LL, Yu JH (2019) 5-Aminolevulinic acid (ALA) biosynthetic and metabolic pathways and its role in higher plants: a review. Plant Growth Regul 87(2):357–374. https://doi.org/10.1007/s10725-018-0463-8
Younis ME, Abdel-Aziz HMM, Heikal YM (2019) Nanopriming technology enhances vigor and mitotic index of aged Vicia faba seeds using chemically synthesized silver nanoparticles. S Afr J Bot 125:393–401. https://doi.org/10.1016/j.sajb.2019.08.018
Zarif F, Khurshid S, Muhammad N, Qureshi MZ, Shah NS (2020) Colorimetric sensing of hydrogen peroxide using ionic-liquid-sensitized zero-valent copper nanoparticle (nZVCu). ChemistrySelect 5(20):6066–6074. https://doi.org/10.1002/slct.202001470
Zengin FK, Kirbag S (2007) Effects of copper on chlorophyll, proline, protein and abscisic acid level of sunflower (*Helianthus annuus* L.) seedlings. J Environ Biol 28(3):561–566
Zhang CP, Li YC, Yuan FG, Hu SJ, Liu HY, He P (2013) Role of 5-aminolevulinic acid in the salinity stress response of the seeds and seedlings of the medicinal plant *Cassia obtusifolia* L. Bot Stud. https://doi.org/10.1186/1999-3110-54-18
Zhang J, Kang Z, Chen J, Du G (2015) Optimization of the heme biosynthesis pathway for the production of 5-aminolevulinic acid in *Escherichia coli*. Sci Rep 5:8584. https://doi.org/10.1038/srep08584
Zhuykov O, Burdiug O, Ushkarenko V, Lavrenko S, Lavrenko N (2020) Photosynthetic activity and productivity of sunflower hybrids in organic and traditional cultivation technologies. Agrolife Sci J 9(1):374–381

Publisher's Note Springer Nature remains neutral with regard to jurisdictional claims in published maps and institutional affiliations.